Exceedance frequency of appearance of extreme internal waves in the World Ocean

Tatyana Talipova[1,2], Efim Pelinovsky[1,2], Oxana Kurkina[1], Ayrat Giniyatullin[1], Andrey Kurkin[1]

[1]Nizhny Novgorod State Technical University n.a. R.E. Alekseev, Nizhny Novgorod, 603950 Russia

5   [2]Institute of Applied Physics, Nizhny Novgorod, 603950 Russia

Correspondence to: Andrey Kurkin (aakurkin@gmail.com)

Abstract. Statistical estimates of internal wave appearance in different regions of the World Ocean are discussed. It is found that the observed exceedance probability of large-amplitude internal waves in most cases can be described by the Poisson curve, which is one of the typical curves of extreme statistics. Detailed analysis is done for the internal waves in the several

10   areas of the World Ocean: tropical part of the Atlantic Ocean, the North-West shelf of Australia, the Mediterranean Sea near the Egyptian Coast and the Yellow Sea.

Keywords: Internal waves, Exceedance frequency, Poisson statistics

1 Introduction

15   Internal waves are observed everywhere in shelf zones of seas. The main source of their generation in the ocean is the semi-diurnal tidal wave, which is initially barotropic and generates the baroclinic tidal wave by the scattering on the continental shelf. As it can be expected, periodic tide generates the regular internal waves each 12.4 hours and this process is well described in literature and modelled numerically, see for instance (Vlasenko et al., 2005). Nevertheless the variability of the magnitude of moon tide and daily temperature and salinity of the sea water lead to random characteristics of the observed

20   internal wave field, see, for example, book by Miropolsky (2001) and review paper by Helfrich and Melville (2006). Popular methods to analyze the random internal wave field are the spectral and correlational methods. As a result, climatic spectra of internal waves have been determined and in particular well-known Garret-Munk climate spectrum (Garret and Munk, 1975), which served as the basis for the regionalization of the World Ocean by the internal wave average parameters. This actually determines the background of the ocean internal waves, over which more intensive processes occur leading to the generation

25   of large (up to extreme values of 500 m) amplitude internal waves (Alford et al., 2015). Data of the large-amplitude internal waves in various areas of the World Ocean are collected in numerous papers (Apel et al., 1985; Salusti et al., 1989; Holloway et al., 1999; Ramp et al., 2004; Sabinin and Serebryany, 2007; Shroyer et al., 2011; Xu and Yin, 2012; Kozlov et al., 2014; Xu et al, 2016). For example, extreme waves of high amplitudes in the Strait of Gibraltar and Kara Gates Strait are analyzed in (Morozov et al., 2002, 2003, 2008). Large-amplitude internal waves cause interest of researchers because of their

dangerous action on offshore platforms (Fraser, 1999; Song et al., 2011), their influence on safety of submarines and underwater vehicles (Osborn, 2010), and an effect on phase fluctuations of acoustic signals at large distances (Warn-Varnas et al., 2003; Rutenko, 2010; Si et al., 2012;). The special warning systems are developed now in regions of high risk of a pipe and platform damage by the intensive internal waves (Stöber and Moum, 2011).

5   Internal waves in the ocean can be considered as a continuous random process, and their large amplitudes can be interpreted as outliers of a random process and can be described by the tails of the probability distribution functions. Consequently, the statistics of these processes is usually different from the Gaussian (normal) distribution. Non-Gaussian character of the observed internal wave field has been mentioned for many areas of the World Ocean (Miropol'sky, 2001; Wang and Gao, 2002). Seasonal and longitudinal statistical analysis of internal wave field has been done recently for the South China Sea
10   (Zheng et al, 2007). It is demonstrated there that the largest number of internal wave packets here is observed at the longitude 116.5ºE (in the latitude band 20-22ºN), and June is the most reach month for the generation of the internal wave packets in the South China Sea. Special analysis of wave amplitude distribution for the tropical part of the western Atlantic Ocean, for the North-West shelf of Australia and the eastern Mediterranean Sea is performed in papers (Ivanov et al., 1993a,b; Pelinovsky et al., 1995), where it is shown that the Poisson law is a good approximation for amplitude distributions
15   of such waves. As it is known Poisson distribution is very popular in the extreme statistics and very often applied in the ocean engineering for description of storm waves (Pelinovsky and Kharif, 2016), tsunamis (Kaistrenko, 2014), rogue waves (Kharif et al., 2009), in geophysics for description of climate anomalies (Dischel, 2017), etc. However, the distribution law for temperature deviations in the tropical part of the eastern Atlantics (Mesopolygon-85) is more close to the Gaussan distribution (Morozov et al., 1998).

20   In the present paper application of methods of extreme statistics to large-amplitude internal waves is briefly reviewed. First, the theoretical approach is revised in Section 2. Then, the results of statistical processing of the internal wave records in various areas of the World Ocean are presented in Section 3. Conclusions are given in Section 4.

2 Extreme statistics methods for high amplitude internal waves

Let $\eta(t,/x,y,z)$ describe the vertical displacement of any isopycnal surface at fixed point, which, in the first approximation,
25   can be considered as stationary random process. Usually, a few central moments

$$\mu_r = \int_{-\infty}^{\infty} (\eta - \overline{\eta})^r P(\eta)d\eta \qquad (r = 2, 3, 4) \tag{1}$$

are computed for the statistical analysis. Here $P(\eta)$ is the probability density function and $\overline{\eta}$ is the mean value

$\overline{\eta} = \int\limits_{-\infty}^{\infty} \eta P(\eta) d\eta$ (unperturbed position of isopycnal surface). The second moment $\mu_2 = \sigma^2$ determines the intensity of internal

wave oscillations and σ is root mean square height of internal waves. The third and fourth moments determine skewness Sk = μ_3/σ^3 and kurtosis $Ku = \mu_4/\sigma^4$, which are used to characterize the deviation of the distribution function from the Gaussian

5   curve (note that $Sk = 0$ and $Ku = 3$ for Gaussian distribution). The sign of the skewness in our opinion can be explained by the specific shape in the internal Stokes wave, which follows from the weakly nonlinear theory of internal waves. In opposite to nonlinear surface waves, which always have narrow and high crests and flat troughs, internal waves on different depths can have either narrow crests and flat troughs or vice-versa depending on the density stratification and modal structure. For more energetic first mode internal waves, the character of the asymmetry of wave profile with respect to the horizontal axis

10   is determined by the coefficient of the quadratic nonlinear term in the Korteweg-de Vries equation, which is strongly variable in the World Ocean (Grimshaw et al., 2007; Kurkina et al., 2011, 2017a,b). Computations of the skewness and kurtosis as well as distribution function of nonlinear internal waves is an interesting problem which is not studied well up to now.

Here we will use the direct method to evaluate the statistics of large-amplitude internal waves. Fixing some value of vertical

15   displacement, we analyze statistics of the exceedance of wave oscillations above this level (outliers of random process). Let us briefly reproduce the well-known approach for calculating the exceedance frequency for continuous processes (Gumbel, 1958; Stuart, 2001) with application to the internal waves.

Internal waves have a vertical structure, and the most energetic lowest-mode waves are more intensive in pycnocline. For definiteness, we chose vertical displacement in the pycnocline and denote it $\eta(t)$ omitting coordinates of the pycnocline in

20   this function. For the outlier beyond the level A in the interval Δt both conditions should be satisfied at once

$\eta(t) < A$ and $\quad \eta(t+\Delta t) > A$. $\hspace{4cm}$ (2)

Due to the smallness of Δt we can represent $\eta(t+\Delta t) \approx \eta(t) + w(t)\Delta t$, where $w(t) = d\eta/dt > 0$ is the vertical velocity of particles lying within the isopycnal surface, and we rewrite condition (2) as

$A - w(t)\Delta t < \eta(t) < A$. $\hspace{4cm}$ (3)

25   The required probability of finding $\eta(t)$ in the interval (3) is

$P(A - w\Delta t < \eta < A) = \int\limits_{0}^{\infty} dW \int\limits_{A-w\Delta t}^{A} f(\eta, W; t) d\eta$, $\hspace{3cm}$ (4)

3

where $f(\eta, w; t)$ is the two-dimensional probability density of vertical displacement $\eta(t)$ and the vertical velocity $w(t)$ at the same moment of time and the same coordinates. Since Δt is small, we can use the mean-value theorem to calculate the inner integral in (4) and, hence

$$P(\eta - w\Delta t < \eta < A) = \Delta t \int_0^\infty wf(A, w; t)dw .$$ (5)

5   Probability density function (in time) can be easily found from (5)

$$p(A; t) = \int_0^\infty wf(A, w; t)dw .$$ (6)

Similarly, the probability of crossing the level A from the top down (into the region of small value of isopycnal displacement) is

$$p'(A; t) = -\int_{-\infty}^0 wf(A, w; t)dw ,$$ (7)

10   since this requires $w < 0$. This equation can be used to calculate probability of large troughs (which can be as danger as large crests) in the vertical displacement. As it is known, large internal waves in the ocean have usually negative polarity and this correlates with negative sign of the quadratic nonlinearity parameter in the weakly nonlinear theory based on the Korteweg-de Vries equation for deepest parts of the World Ocean (Grimshaw et al, 2007).

Here we calculate the average number of "positive" outliers (large crests) in wave record. To do so we divide the total time

15   interval into small subintervals Δt_j and introduce a random value N_j equal to 1 for an outlier and 0 outside the outlier. Then the total number of outliers is $N(A) = \sum N_j$ and its mean value is the ensemble average, the probability of this is equal to the probability of crossing the level (6). Moving on to the limit for $\Delta t_j \to 0$, we finally have

$$<N(A)> = \int_0^T \int_0^\infty wf(A, w; t)dwdt .$$ (8)

In the case of a stationary random process the formula (8) is simplified

20    $$<N(A)> = T \int_0^\infty wf(A, w)dw .$$ (9)

Thus, the average number of outliers is proportional to the time interval and decreases with the increase in the outlier level. The same approach can be used to compute average number of "negative" outliers (the deepest troughs) in the internal wave field.

4

Only the average number of outliers was discussed above without considering their probabilistic distribution. A much more difficult problem is to calculate the latter. It should be noted that if outliers are rather rare (which is typical for very large-amplitude internal waves, $A \to \infty$), then their distribution can be regarded as Poisson one. Then the probability of at least one outlier occurred in the time interval t is

5    $P = 1 - \exp(-\nu t)$,   (10)

where the mean frequency of outliers $\nu = <N>/T$, is found from (9) as

$$\nu(A) = \int_0^\infty w f(A, w) dw.$$ (11)

The average frequency of outliers in the first approximation can be used as an estimate of the internal wave exceedance (cumulative) frequency with the amplitudes greater than the given value of A.

10   Detail calculations of the outlier characteristics in the internal wave field require the knowledge of two-dimensional (vertical displacement and vertical velocity) distribution functions of isopycnal variation which are usually not measured. If the internal wave random field is assumed to be normal, the density of distribution function is described by a Gaussian curve

$$f(\eta) = \frac{1}{\sqrt{2\pi}\delta} e^{-\frac{(\eta - \bar{\eta})^2}{2\delta^2}},$$ (12)

where δ is the standard deviation (mean amplitude of the internal waves). The distribution function of the vertical

15   displacement and the vertical velocity for the normal process do not correlate, so their two-dimensional probability density splits into a product of two Gaussian curves (12) with naturally different mean-square deviations. Then the average frequency of outliers is

$$\nu(A) = \frac{\delta_w}{2\pi\delta_\eta} \exp(-\frac{A^2}{2\delta_\eta^2}),$$ (13)

where δ_w is the mean-square (standard deviation) value of the vertical velocity in the internal wave and δ_η is the mean-square

20   value of the vertical isopycnic displacement. Thus, the internal wave exceedance frequency depends on the wave amplitude according to the Gaussian curve, which rapidly decreases with increasing amplitude. We will demonstrate Gaussian character of cumulative frequency for tropical zone of eastern Atlantic Ocean.

One should remember that usually internal wave field statistical distributions in the areas of the World Ocean differ from normal distribution as we have already pointed in Introduction, see book by Miropolsky (2001), so the result will be different

25   from (13) depending on the particular form of the tails of the distribution function in large amplitude range. As it was shown

in (Leadbetter et al., 1983), the intermediate asymptotic exceedance frequency for large outliers has the form of a Poisson curve

$$\nu = \nu_0 \exp\left(-\frac{A}{A_0}\right),$$ (14)

where ν_0 and A_0 are the parameters depending on the specific type of "tails" of the distribution function in the large amplitude range. This expression can be used to compute exceedance (cumulative) frequency of large outliers (positive or negative) in the internal wave field. Obviously, the predicted amplitude values are also random, and here one can speak only about its evaluation. So, to estimate the predicted amplitude A it is necessary to set the value of the exceedance frequency

$$\nu = 1/T,$$ (15)

where T is the prediction time (or the recording time). Expression (14) is used to calculate the design amplitude A of internal wave on prognostic time interval T

$$A_T = A_0 \ln(\nu_0 T).$$ (16)

Characteristic values of A_0 and ν_0 are different for various areas of the World Ocean and will be discussed in the next section.

3 Statistics of internal wave field

3.1. Probability density function in the Yellow Sea

The shallow water (Qingdao offshore area) experimental data from the Yellow Sea are processed by (Wang and Gao, 2002). The thermistor chain was used for measurements. The temporal lengthscale of records is 49 h 49 min with sampling interval 6.4 s. The water depth is 33 m. Rather narrow undisturbed pycnocline lies from 10 m to 16 m with maximum of the Brunt-Vaisala frequency $N_{max} = 0.067$ s^{-1}. Vertical displacements (not the amplitudes!) of highpass-filtered 25º - 17.5º (16 levels) isotherms are described and their histograms are plotted. The maximum wave height here is not more than 5 m, nevertheless the process differs from the Gaussian process. It is found that the standard deviation is slowly growing from 0.46 m to 0.56 m from surface to bottom. Skewness is negative for each isotherm and has the maximum of 0.5 in absolute value at the depth 15 m with 0.36 at the surface and 0.06 close to bottom. Kurtosis changes from 3.24 close to the bottom to 5.05 at the depth of 14 m and 4.12 near the surface. It is shown that the distribution of large internal wave amplitudes do not coincide with Gaussian distribution.

We can explain the sign of the computed skewness applying the weakly nonlinear theory of internal waves based on the Korteweg-de Vries equation (Pelinovsky and Shurgalina, 2017). For given area in the Yellow Sea the sign of quadratic nonlinear term in this equation is negative, because the water stratification (see in Wang and Gao, 2002) is practically two-

layer with pycnocline situated above the half-depth (Djorjevich and Redekopp, 1978; Kakutani and Yamasaki, 1978). Nonlinear waves as solutions of the extended Korteweg-de Vries equation with negative quadratic nonlinearity have deeper troughs, for instanceinternal solitons have negative polarity (Grimshaw et al., 2007). This leads to the negative values of the skewness.

3.2 Exceedance frequency of internal waves in the tropical zone of western Atlantic

The exceedance frequency of internal waves is estimated using data obtained during the 39th cruise of the RV "Akademik Vernadsky" in the north-western Atlantic Tropical Zone near the mouth of the Amazon River, 2-15° N, 38-52° W (Ivanov et al., 1993b). Internal waves of average amplitudes from 2.5 to 10 m were observed in this region. To obtain long-term internal wave recordings the ship echo sounder was used. It allows for studying sound-scattering layer fluctuations at depths up to 100 m. These fluctuations are known to be due to various causes, but in the range up to 3 hour wave periods they are mainly related to internal waves. The wave period also varies over a wide range from 3 min to 30 min on the sonar recordings. Since the measurements were made on the ship moving at a velocity of about $V = 15$ knots and as the maximum of internal wave speed is $c = 3$ knots in order of magnitude, the internal wave pattern can be considered frozen in the first approximation. In this case, the "true" wave period increases in comparison to the observed one with ratio $V/c = 5$. The amplitude of sound-scattering layer fluctuations was everywhere identified with the internal wave amplitude in the pycnocline. The total recording duration was about 218 hours. Wave height (defined as the fluctuation swing between adjacent extremes) and fluctuation duration on the recording were adopted as the main characteristics. Primary results of daily echogram processing are presented in the paper (Ivanov et al., 1993b). These data are used to estimate the exceedance (cumulative) frequency. They agree well with the regression line

$$\nu = 9.2 \exp(-0.3H) \,, \tag{17}$$

where H is wave height measured in meters, and the dimension for v is [hr^{-1}], except for the heights greater than 25 m, where the total number of wave observations does not exceed six. Expression (17) is used to estimate the predicted wave height versus a forecast time function

$$H = 18 + 3.3 \ln T \,. \tag{18}$$

Predicted values of internal wave heights versus time are summarized in Table 1.

During the time spent at the area, the "true" internal wave recording time (considering the ship movement) was about 45 days. According to the prediction for this period, a wave with a height of more than 31 m should be observed once, with a height of more than 27 m – twice, and more than 23 m – three times. In fact, the level of 31 m was exceeded three times, and the level of 27-28 m - six times, and this is quite well within the framework of predictive models.

3.3 Internal wave temperature at Mesopolygon-85 in the Atlantic Ocean

The wave process in the open ocean can be expected closer to normal, which makes it possible to use the theory of normal random process and estimate the limits of its applicability in internal wave practice. In the present paper the exceedance frequency analysis is undertaken for internal wave records obtained from buoys in the area in the eastern Atlantic Ocean in 1985 (Mesopolygon-85; the detailed description of the experiment is given in Kort, 1988). Seventy-six moorings with current and temperature meters were deployed in the study area called Mesopolygon- 85 in the eastern part of the Atlantic Ocean with the objective of studying mesoscale variability of hydrophysical processes. The area was located at the juncture of the Canary Basin and the Cabo Verde Basin (19-21°N and 36-38°E). The buoy stations operated approximately two months from April to May. The measuring devices were placed on four levels, but the most representative measurements were made at the level of 200 m. The total size of the area was approximately 80 to 80 miles. The sampling interval was 15 min. In the Mesopolygon area, the bottom is covered with hills from 500 to 1000 m high over the floor. Such hills are located every 10 or 20 miles. They form a corrugated bottom topography over which the horizontal streamlines of barotropic currents are deformed. Thus, the internal tide is generated immediately in this area over the deep-sea bottom topography. It should be mentioned that 49 buoy records are processed there, and it is a unique possibility to estimate the horizontal variability of the internal wave amplitude distribution function.

Recordings of temperature variations (in centigrades) at various points of the area were used to calculate the average frequency of outliers (temperature variation exceeding the fixed value ΔT). All processed records are very well described by a Gaussian distribution

$$\nu = (0.79 \pm 0.17)\exp\left(-(10.61 \pm 4.5)(\Delta T)^2\right), \tag{19}$$

where the parameters vary from station to station. Here ν again has the dimension of hr^{-1} and ΔT is in centigrade. It should be noted that the deviation in ν_0 are from 21% to 42% in the exponent, on the area about 48000 km^2 in the tropical part of eastern Atlantic. More details of the experiment data are given in (Morozov et al., 1998).

3.4 Internal wave heights in the Mediterranean Sea

Let us discuss internal wave appearance in micro-tidal seas, where one can expect the universe statistical characteristics over a short period of time without being tied to the phases of the moon. The mechanisms of internal wave generation here may be such as storms and upwelling as well as the effect of river flow in mouth. Internal wave observations for one of the Mediterranean regions (the Levant Sea) obtained during the 27th cruise of the RV "Professor Kolesnikov" (July-August 1991) are used in the paper. These old data briefly presented in (Ivanov et al. 1993a) are now revised. During the period from 27 to 29 July, 1991 a special experiment to record internal waves was performed at the area near the Egyptian shelf. The probe by MHI 4106 (temperature sensor of 25 meters length) had been dragged in tacks crossing as a star. The data of temperature were later recalculated into the vertical isopycnal displacements. The measurements were carried out in a

thermocline. The basin depth at the area s varies from 200 to 1100 m. The vertical profile of the Brunt-Vaisala frequency contains the pycnocline at a depth of about 25 m at a frequency of 17 cycle/hour. Below the pycnocline the mean value of the Brunt-Vaisala frequency was about 4 cycle/hour. The wave height distribution function is calculated from these data. The vessel speed was approximately $V = 5$ knots, which significantly exceeds the internal wave propagation speed in this region ($c = 2$ knots). Therefore, in the first approximation, the internal wave field can be considered as frozen. This means that the "true" time recording can be increased by $V/c = 2.5$ times. The applicability of Gaussian (red) and Poisson (blue) laws for the exceedance (cumulative) frequency, as one see from Fig. 1, is well applicable to the observed data: they are approximated by the formulas

$$\nu = 4\exp(-1.9A), \text{ (a)} \qquad \qquad \nu = 2\exp(-A^2) \quad \text{(b)} \qquad \qquad \qquad (20)$$

where A is a wave amplitude measured in meters, and ν is in hr^{-1}. The obtained distribution (20) can be used for the prediction of relatively large amplitude waves. The predicted values of internal wave amplitudes calculated using formula (20a) that can occur in the Mediterranean Sea near the Egyptian shelf over different time periods, are summarized in Table 2.

It should be noted that the observed internal waves at this region have much smaller amplitudes than on the ridges, for example the Mascarene Ridge (Morozov et al., 1996) or in the Luzon Strait where 100-meter waves are recorded (Ramp et al., 2004). This fact is well known for the micro-tidal seas and is reflected in the large value of the return period for internal wave of 5 m amplitude in this part of the Mediterranean Sea. This is why the observed height distribution is between Gaussian statistics (for weak-amplitude waves) and Poisson statistics (for large-amplitude waves).

3.5 Exceedance frequency in the current velocity from the data of buoy stations (the north-western shelf of Australia)

Relatively long internal wave recordings were obtained at buoy stations on the northeastern shelf of Australia (Pelinovsky et al., 1995). The water depth is approximately 123 m. Flow velocities in the internal wave range, recorded at a level of 3 m above the ocean bottom, will be analyzed in the present paper. Measurements were taken every 2 minutes for 10 days. Only the flow component, which contains the strongest wave fluctuations, was analyzed in the direction transverse to the isobaths (45^0 north - east). The time series passed through a high-frequency filter to remove the tidal component. Each recording is divided into equal intervals of 4000 minutes. Primary time series processing results are given by Pelinovsky et al. (1995). The calculated values of exceedance frequency for different amplitudes are approximated by the expression

$$\nu = 1.33\exp(-0.071U), \qquad \qquad \qquad (21)$$

where ν has the dimension of hr^{-1} and amplitude of horizontal velocity variation U is in cm/sec.

The regression formulae obtained above can be used for calculation of exceedance probability of large-amplitude internal waves as function of wave flow amplitude and time duration. Result of calculation for the North West Shelf of Australia is represented in Fig. 2.

4 Conclusions

Here we have considered statistical characteristics of the internal wave field in several zones of World Ocean: the tropical part of the western Atlantic Ocean near the Amazonian mouth, the part of the eastern Atlantic, the west part of Mediterranean Sea, the North West shelf of Australia and the Yellow Sea shelf (Fig. 3).

5   It is difficult directly to compare the results of exceedance frequency calculations for various regions of the World Ocean. The main difficulty of the comparison is that different characteristics were measured. In particular, in the tropical zone of the Atlantic, the vertical displacement of the sound-scattering layers was measured, in the Mediterranean Sea it was the amplitude of displacement of the thermocline, while on the Australian shelf the records of flow velocity fluctuations were analyzed, and at the Mesopolygon-85 it was the temperature fluctuations on a given level. The internal mode structures were

10 never analyzed for these measurements, and we cannot confirm that the observations are done in the mode maximum. So, we may predict the internal wave amplitude only at the level of measurements. Also for three analyzed areas the Poisson law is valid for internal wave amplitude distribution, but for Mesopolygon - 85 we get the Gauss distribution what is more appropriate for very small amplitudes. Nevertheless, the internal waves in the eastern Mediterranean Sea have amplitudes not more than 2 m but the amplitude distribution function is closer to the Poisson law. It seems, all mentioned above is the

15 subject for following investigations. Meanwhile, the value of ν_0 has universal character and should not depend on the measured characteristics of internal waves. For the Australian shelf $\nu_0 = 1.3$ hr^{-1}, for the tropical zone of the Atlantic $\nu_0 = 9.2$ hr^{-1}, for Mesopolygon-85 $\nu_0 = 0.8$ hr^{-1} and for the Mediterranean (Levant Sea) $\nu_0 = 4$ hr^{-1}. These values turned out to be very heterogeneous. It should be the feature of the ocean region. We can attribute this difference to the intensity of internal wave generation in various regions of the ocean. It is known that tropical South Atlantic is a region of large - amplitude

20 internal waves due to strong generation of internal tides by the interaction between the barotropic tide and bottom topography (Morozov, 1995) . Low amplitude but often-generated internal waves are performed near the Nile River mouth. Internal waves are generated mainly by tide propagating across the Australian shelf. We may proposeassume, as $\nu_0 = 0.8$ hr^{-}, that internal waves of high amplitudes are not often recorded in the region of Mesopolygon-85, but ordinary internal waves are always generated.

25 Currently, the numerical methods to predict internal wave field characteristics in different areas of the World Ocean are widely applied. Calculations demonstrate that their characteristics are very sensitive to the density stratification of the ocean. The influence of variation of water stratification on the internal wave dynamics can be illustrated by the seasoning maps of kinematic parameters of internal waves (Kurkina et al., 2001, 2017a,b). Computing many scenario of the internal wave developing for various hydrological conditions, some statistical estimates can be done. Such computations have been done

30 already within the Euler equations for stratified water for the Barents Sea (Kurkina and Talipova, 2011; Talipova et al., 2014), the Sea of Okhotsk (Kurkina et al., 2017b) etc.

10 **References**

Alford, M.H., Peacock, T., MacKinnon, J.A., Nash, J.D., Buijsman, M.C., Centurioni, L.R., Chao, S.Y., Chang, M.H., Farmer, D.M., Fringer, O.B., Fu, K.H., Gallacher, P.C., Graber, H.C., Helfrich, K.R., Jachec, S.M., Jackson, C.R., Klymak, J.M., Ko, D.S., Jan, S., Johnston, T.M.S., Legg, S., Lee, I.H., Lien, R.C., Mercier, M.J., Moum, J.N., Musgrave, R., Park, J.H., Pickering, A.I., Pinkel, R., Rainville, L., Ramp, S.R., Rudnick, D.L., Sarkar, S., Scotti, A., Simmons, H.L., St Laurent,

15 L.C., Venayagamoorthy, S.K., Wang, Y.H., Wang, J., Yang, Y.J., Paluszkiewicz, T., and Tang, T.Y.: The formation and fate of internal waves in the South China Sea, Nature, 521, P. 65-69, 2015,

Apel, J.R., Holbrock, J.R., Kiu, A.K., and Tsai, J.J.: The Sulu Sea internal soliton experiment, J. Phys. Oceanogr., 15, 1625-1651, 1985.

Dischel, R.S., (Ed): Climate Risk and the Weather Market, Incisive Risk Information (IP) Limited, 2017.

20 Djordjevic, V.D., and Redekopp, L.G.: The fission and desintegration of internal solitary waves moving over two-dimensional topography, J. Phys. Oceanogr., 8, 1016-1024, 1978.

Fraser, N.: Surfing an oil rig, Energy Rev., 20(4), 1999.

Garrett, C.G.R., and Munk, W.H.: Space-time scales of internal waves: a progress report, Jour. Geophys. Res., 10(3), 291-297, 1975.

25 Grimshaw, R., Pelinovsky, E., and Talipova, T.: Modeling internal solitary waves in the coastal ocean, Survey in Geophysics, 28(2), 273-298, 2007.

Gumbel, E.J.: Statistics of Extremes, Columbia Univ. Press, New York, 384, 1958.

Helfrich, K.R., and Melville, W.K.: Long Nonlinear Internal Waves, Annu. Rev. Fluid Mech., 38, 395-425, 2006.

Holloway, P., Pelinovsky, E., and Talipova, T.: A generalised Korteweg-de Vries model of internal tide transformation in the

30 coastal zone, J. Geophys. Res., 104, 18333-18350, 1999.

Ivanov, V.A., Pelinovsky, E.N., and Talipova, T.G.: Recurrence Frequency of Internal Wave Amplitudes in the Mediterranean, Oceanology, 33(2), 180-184, 1993a.

Ivanov, V.A., Pelinovsky, E.N., and Talipova, T.G. The long-time prediction of intense internal wave heights in the tropical region of Atlantic, J. Phys. Oceanography, 23(9), 2136-2142, 1993b.

Kaistrenko, V.: Tsunami, Recurrence Function: Structure, Methods of Creation, and Application for Tsunami Hazard Estimates, Pure Appl. Geophys.,171, 3527-3538, 2014.

Kakutani, T., and Yamasaki, N.: Solitary waves on a two-layer fluid, J. Phys. Soc. Japan, 45, 674-679, 1978.

Kharif, Ch., Pelinovsky, E., and Slunyaev, A., Rogue Waves in the Ocean, Springer, 216, 2009.

Kozlov, I., Romanenkov, D., Zimin, A., and Chapron, B.: SAR observing large-scale nonlinear internal waves in the White Sea, Remote Sensing of Environment, 147, 99-107, 2014.

Kurkina, O., and Talipova, T.: Huge internal waves in the vicinity of Spitsbergen Island (Barents Sea), Natural Hazards Earth System Sciences, 11, 981–986. 2011.

Kurkina, O., Talipova, T., Pelinovsky, E., and Soomere, T.: Mapping the internal wave field in the Baltic Sea in the context of sediment transport in shallow water, J Coastal Research, SI, 64, 2042-2047, 2011.

Kurkina, O., Rouvinskaya, E., Talipova, T. and Soomere, T.: Propagation regimes and populations of internal waves in the Mediterranean Sea basin, Estuarine, Coastal and Shelf Science, 185, 44-54, 2017a.

Kurkina, O.,, Talipova, T. , Soomere, T., Kurkin, A., and Rybin, A.: The impact of seasonal changes in stratification on the dynamics of internal waves in the Sea of Okhotsk, Estonian Journal of Earth Sciences, 66(4), 238-255, 2017b.

Kort, V.G. (Ed.): Hydrophysical studies on the program "Mesopolygon", M., Nauka, 1988.

Leadbetter, M.R., Lindgren, G., and Rootzen, H.: Extremes and Related Properties of Random Sequences and Processes, Springer, 1983.

Miropolsky, Yu. Z.: Dynamics of internal gravity waves in the ocean, Kluwer Academic Publishers, Boston, 421, 2001.

Morozov E.G. Semidiurnal internal wave global field, Deep Sea Research, vol. 42, No 1, 1995, 135-148

Morozov E.G., Vlasenko V.I. Extreme tidal internal waves near the Mascarene Ridge. J.Marine Systems, V.9 (3-4), p. 203-210, 1996

Morozov, E., Pelinovsky, E., and Talipova, T.: Exceedance Frequency for Internal Waves during the Mesopolygon-85 Experiment in the Atlantic, Oceanology, 38(4), 470-475, 1998.

Morozov E.G., Trulsen K., Velarde M.G., and Vlasenko V.I., Internal tides in the Strait of Gibraltar, J. Physical Oceanography, vol. 32, 3193-3206, 2002.

Morozov E.G., Parrilla-Barrera G., Velarde M.G., Scherbinin A.D., The Straits of Gibraltar and Kara Gates: A Comparison of Internal Tides, Oceanologica Acta, Vol. 26 (3), 231-241, 2003.

Morozov E.G., Paka V.T., Bakhanov V.V., Strong internal tides in the Kara Gates Strait, Geophysical Research Letters, p. L16603, 2008.

Osborne, A.: Nonlinear Ocean Waves and the Inverse Scattering Transform, Academic Press, 944, 2010.

Pelinovsky, E., Holloway, T., and Talipova, T.: A statistical analysis of extreme events in current variations due to internal waves from the Australian North West Shelf, J. Geophys. Res., 100(C12), 24831-24839, 1995.

Pelinovsky, E., and Kharif, C. (Eds): Extreme Ocean Waves. 2d Edition, Springer, 236, 2016.

Pelinovsky, E., and Shurgalina, E.: KDV soliton gas: interactions and turbulence. Book: Challenges in Complexity: Dynamics, Patterns, Cognition (Eds: I. Aronson, N. Rulkov, A. Pikovsky, L. Tsimring), Series: Nonlinear Systems and Complexity, Springer, 20, 295-306, 2017.

5   Ramp, S.R., Tang, T.Y., Duda, T.F., Lynch, J.F., Liu, A.K., Chiu, C.S., Bahr, F.L., Kim, H.R., and Yang, Y.J.: Internal solitons in the northeastern South China Sea - Part I: Sources and deep water propagation, IEEE J. Ocean. Eng., 29(4), 1157-1181, 2004.

Rutenko, A.N.: The influence of internal waves on losses during sound propagation on a shelf, Acoustical Physics, 56, 703-713. 2010.

10   Sabinin, K.D., and Serebryany, A.N.: "Hot Spots" in the Field of Internal Waves in the Ocean, Acoustical Physics, 53(3), 357-380, 2007.

Salusti, F., Lascaratos, A., and Nittis, K.: Changes of polarity in marine internal waves: Field evidence in eastern Mediterranean Sea, Ocean Modelling, 82, 10-11, 1989.

Shroyer, E.L., Moum, J.N., and Nash, J.D.: Nonlinear internal waves over New Jersey's continental shelf, J. Geoph. Res.,
15   116, C03022, 2011.

Si, Z., Zhang, Y., and Fan, Z.: A numerical simulation of shear forces and torques exerted by large-amplitude internal solitary waves on a rigid pile in South China Sea, Appl. Ocean Res., 37, 127-132, 2012.

Song, Z.J., Teng, B., Gou, Y., Lu, L., Shi, Z.M., Xiao,Y., and Qu, Y.: Comparisons of internal solitary wave and surface wave actions on marine structures and their responses, Applied Ocean Research, 33, 120-129, 2011.

20   Stöber, U., and Moum J.N.: On the potential for automated realtime detection of nonlinear internal waves from seafloor pressure measurements, Appl. Ocean Res., 33, 275-285, 2011.

Stuart, C.: An Introduction to Statistical Modeling of Extreme Values, Springer, 242, 2001.

Talipova, T.G., Kurkina, O.E., Terletska, E.V., Kurkin, A.A., and Rouvinskaya, E.A.: Modeling of internal wave field in the coastal zone of the Barents Sea, Ecological Systems and Devices, 3, 26-38, 2014.[in Russian]

25   Xu, J., Chen, Zh. , Xie, J.,. and Cai, Sh.: On generation and evolution of seaward propagating internal solitary waves in the north western South China Sea, Commun Nonlinear Sci Numer Simulat, 32, 122-136, 2016.

Xu, Zh., and Yin, B.: Variability of Internal Solitary Waves in the Northwest South China Sea, Oceanography, Prof. Marco Marcelli (Ed.), ISBN: 978-953-51-0301-1, InTech., 2012.

Vlasenko, V., Stashchuk, N., and Hutter, K.: Baroclinic Tides: Theoretical Modeling and Observational Evidence,
30   Cambridge University Press, 351, 2005.

Wang, T., and Gao, T.: Statistical properties of high-frequency internal waves in Qingdao offshore area of the Yellow Sea, Chinese Journal of Oceanology and Limnology, 20(1), 16-21, 2002.

Warn-Varnas, A. C., Chin-Bing, S.A., King, D. B., Hallock, Z., and Hawkins, J.A. Ocean-acoustic solitary wave studies and predictions", Surveys in Geophysics, 24, 39-79, 2003.

Zheng, Q., Susanto, R.D., Ho, Ch.-R., Song, Y.T., and Xu, Q.: Statistical and dynamical analyses of generation mechanisms of solitary internal waves in the northern South China Sea, J. Geophys. Res., 112, C03021, 2007.
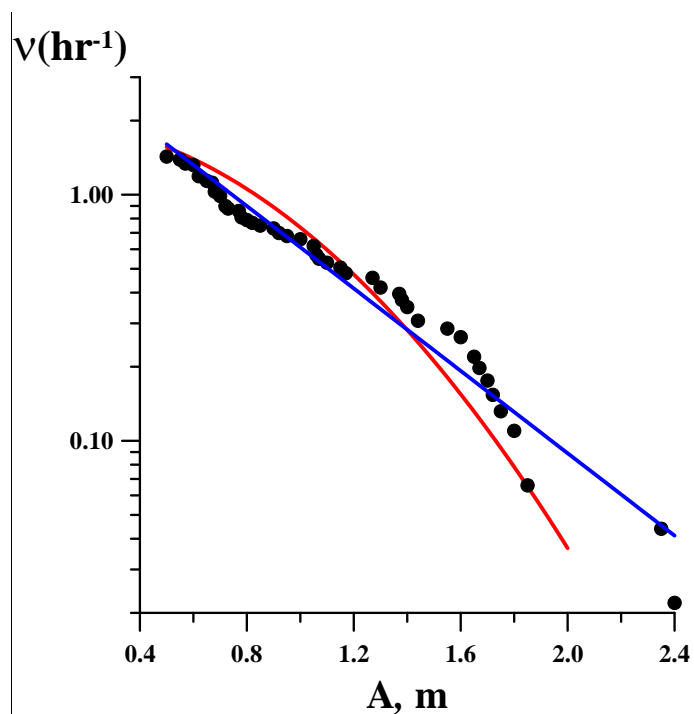
5   **Figure 1: The exceedance frequency of internal wave amplitudes in the eastern part of the Mediterranean Sea.**
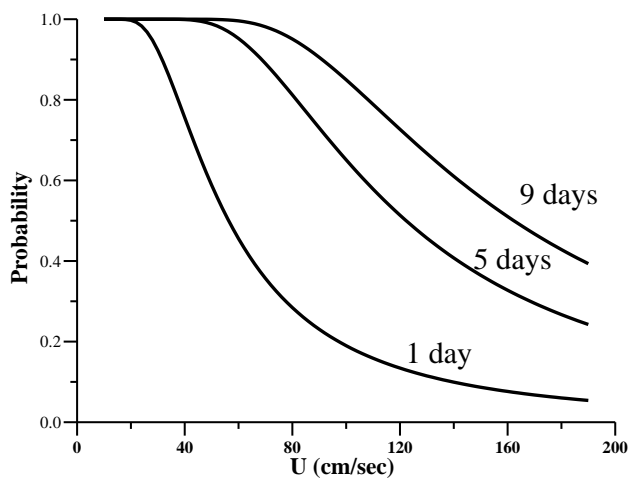

Figure 2: Probability of occurrence of internal waves at the North West Australian shelf.
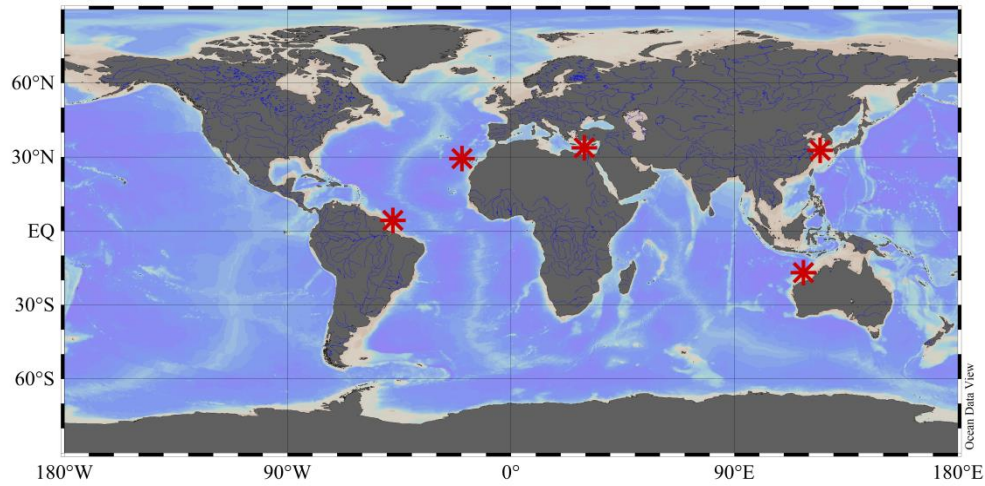
Figure 3: Areas, where we consider statistical characteristics of internal waves.

Table 1: Wave height prediction for the Atlantic tropical zone.

time	1 day	10 days	1 month	3 months	6 month	1 year
H(m)	18	26	29	33	35	38

5

Table 2: Predicted internal wave heights in the Mediterranean Sea.

Time period	1 day	1 week	1 month	3 months
A(m)	2.6	3.6	4.5	5.1